

Response Surface Modelling of the Mechanical Properties of Oil Palm Empty Fruit Bunch Fibre Reinforced Polyester Composites

Chinwe Evangeline Kamma^{1*}

¹*Department of Sustainable Environment and Energy Systems, Middle East Technical University, Northern Cyprus Campus 99738 Kalkanli Guzelyurt via Mersin 10 Turkey*

*Corresponding Author: kammachie@gmail.com

(Received 02-09-2022; Revised 16-09-2022; Accepted 21-09-2022)

Abstract

This work presents a systematic approach to evaluate and study the effect of fibre aspect ratio and fibre volume fraction on the tensile strength, ultimate elongation, modulus of elasticity, strength and impact energy of oil palm empty fruit bunch fibre reinforced polyester composites. Hand-lay-up technique was used in the fabrication of the composite materials. Response surface methodology was used to study the effect of the selected factors on the mechanical properties of oil palm empty fruit bunch fibre reinforced polymer-based composite. The optimum fibre aspect ratio and fibre volume fraction for each mechanical property was determined. From the result of optimization, the maximum value for tensile strength obtained was 12.15N/mm^2 at a fibre aspect ratio of 64 and fibre volume fraction of 26%. The maximum value for ultimate elongation was obtained as 1.939% at a fibre aspect ratio of 124 and fibre volume fraction of 50%, the maximum value for modulus of elasticity was obtained as 1509 N/mm^2 at a fibre aspect ratio of 124 and 34% volume fraction. The maximum value for toughness was obtained as 0.12 N/mm^2 at a fibre aspect ratio of 89 and a volume fraction of 30%. The maximum value of impact energy was obtained



d as 307.72J/m (5.77ft-lbs/in) at 28% fibre volume fraction and an aspect ratio of 69. The maximum value of impact strength was obtained as 4.57N/mm² at a 36% volume fraction and an aspect ratio of 64.

Keywords: Polyester Composites, Response Surface Model, Mechanical Properties, Oil Palm Empty Fruit Bunch

1 Introduction

Polymer matrix composites are composed of a variety of lengths of fibres bonded by a polymer matrix [1]. They are designed such that the mechanical loads to which the structure is subjected in service are supported by the reinforcement. According to [2], composites are materials that consist of two or more chemically and physically different phases separated by a distinct interface. The different systems are combined such that a system is achieved in which useful structural or functional properties are non-attainable by any of the constituents alone.

The wake of engineers' uses of composites started when it was discovered that they have great advantages above steel and its alloys such as low weight and higher resistance, high fatigue strength and faster assembly [3, 4].

Composites are used extensively as materials in making aircraft, electronic devices, packaging, vehicles, home building, etc. They comprise the matrix and reinforcing materials and their use until now has been more traditional than technical. They have served many useful purposes for a long but the application of the material for the utilization of natural fibres as reinforcement in polymer matrix took place quite recently [3]. These natural fibres have advantages such as low density, low cost, low weight, high toughness, acceptable specific length recovery, biodegradability and enhanced energy recyclability [5, 6].

The fruit bunches which are by-products of oil processing are presently industrial wastes. The oil palm empty fruit bunch can be found littered everywhere in oil palm producing areas of Nigeria since the wastes have presently no industrial application. Recently, because of the environmental impact of using oil palm empty fruit bunch as

fuel has been discouraged in Nigeria [18]. Its handling in the oil mills consumes energy. However, oil palm empty fruit bunch used locally to prepare local delicacies like ukwa (breadfruit), ugba (oil bean salad), abacha (slice cassava, popularly called African salad), and in rare cases now, in the production of local black soap because of the large potassium content of the bunch. This study hopes to help find a place for the usefulness of oil palm empty fruit bunch as fibre reinforcement for composites.

Several factors affect the performance of natural fibre reinforced polymer composites such as fibre-matrix adhesion properties, fibre length, fibre volume fraction, and fibre aspect ratio [7]. Composites are generally a combination of heterogenous materials [21], thus to improve the fibre-matrix interaction and adhesion, the fibre is mercerized to remove certain impurities and reduce the hydrophilic characteristics of the fibre leaving the fibre with a rough surface [4, 8-16]. The mixing procedures, type of compatibilizers, and processing and treatment conditions of fibres and the polymer resin have been shown to affect the quality of interfacial bonding between the fibre and the resin [17, 18]. Recent work conducted by Athijayamani et al. highlighted the effects of fibre length and content on composite tensile and flexural strength. The study showed that the tensile and flexural strength of a hybrid roselle/sisal polyester composite increased with increased fibre length and fibre content, while the impact strength reduced correspondingly [19].

Sapuan et al. studied the mechanical properties of woven banana fibre reinforced epoxy composites and found that the composites can be used for household utilities [20]. The industrial potentials of oil palm empty fruit bunch have not been well addressed in the literature to our knowledge. Therefore, the purpose of this work is to evaluate the tensile, and impact strength of short random oil palm empty fruit bunch fibre reinforced polyester composites for application in the automobile industry.

The high demand for low density, low cost, high impact resistance, and renewable and biodegradable materials have led to many works and research on fibre-reinforced polymer composites. However, there has not been rife work in modelling and optimization of the mechanical properties of oil palm empty fruit bunch fibre reinforced polyester composites concerning their fibre aspect ratio and volume traction using the response surface model.

This work hopes to address the above limitation by studying the effect of fibre aspect ratio and fibre volume fraction of oil palm empty fruit bunch fibre reinforced polyester composites on the mechanical properties and modelling the mechanical properties of oil palm empty fruit bunch fibre reinforced polyester composites using surface response technology to determine the optimum fibre aspect ratio and volume fraction for optimum mechanical performance.

2 Research Methodology

A brief description of the materials and methods to be used for the preparation of composites is given in this section. The chemicals to be used for various fibre treatments are discussed. A brief description of the different analytical techniques to be used for the characterization of fibres and composites is also given in this section.

2.1 Oil Palm Empty Fruit Bunch Fibre (RPF)

The Oil Palm Empty Fruit Bunch Fibre used in this work was obtained from the eastern part of Nigeria where the crop is grown for consumption as well as for commercial use.

2.2 Unsaturated polyester resin

General Purpose-grade Unsaturated polyester resin (HSR 8113M), was obtained from Nycil Industrial Chemicals, Ota, Ogun State Nigeria.

2.3 Chemicals for fibre modification

The Sodium hydroxide used for fibre surface modification is of reagent grade and was obtained from new concepts laboratories Obinze, Imo state, Nigeria.

2.4 Fibre preparation and surface modification

Extraction of the OPEFBF and preparation was carried out as follows: The fruits from the bunch were extracted mechanically leaving behind an empty fruit bunch, which was then retted utilizing tank water retting for about three days, and the fibres so obtained were sun-dried.

2.4.1. Mercerization

For preparing randomly oriented oil palm empty fruit bunch fibre composites, the fibres were treated with NaOH of 6wt% at 90mins at room temperature. Finally, the fibres were repeatedly washed and then dried in air and oven. Fibres of an average diameter of 0.41mm and fibre volume fractions of 10%, 20%, and 30% and fibre aspect ratios of 24.39, 73.171, and 121.9512 were obtained.

2.4.2 Preparation of OPEFBF-polyester reinforced composites and test specimens

Randomly oriented OPEFBPF-polyester composites containing fibres of specific length and fibre volume fraction were prepared by hand lay-up method using a stainless steel sheet female mould with a marble tile male mould. Before the composite preparation, the mould surface was polished well and a mould-releasing agent (mirror-glaze) was applied to the surface of the mould. General unsaturated polyester resin (GP) was mixed with 5% by vol. MEKP accelerator and 10% by vol. cobalt naphthenate catalyst. The fibre material was then placed in the mould and the resin mixture was poured evenly on it. After which the mould was closed and the excess resin allowed to flow out as a 'flash' by pressing, the pressure was held constant during the curing process at room temperature for 24 hours. The composite sheet will then be post-cured at 80°C for 4 hours. Test specimens according to ASTM standards were cut out from the sheet.

2.5 Mechanical property measurements: The standard mechanical properties were determined by the procedures found in ASTM (American Society for Testing and Materials) standards for plastics. The mechanical property tested for in this work is ultimate tensile strength and impact strength.

2.5.1 Tensile properties

The tensile properties were tested at the Civil Engineering Laboratory, University of Nigeria, Nsukka (UNN), using a Hounsfield Monsanto Universal Tensometer Machine. The Hounsfield Tensometer is a universal testing machine capable of testing metals,

plastics, textiles, timber, composites, fibres, papers etc. Provisions are made for such tests as tensile, compression, flexural or bending, shear, hardness etc. an important feature of the equipment/machine is the ease with which an auto-graphic record can be made. It contains a spring beam with ranges that are readily interchangeable and used in conjunction with special attachments. This enables tests to be performed on a wide variety of materials. Like most testing machines, the load is applied at one end and the magnitude of the load is measured at the other. The test piece, held in suitable chucks fixed to the spherically seated nosepieces by the chucks attachment pins, is loaded either by hand or employing a motor-driven unit through a worm gearbox. This causes the operating screw to move to the right and so transmits pull to the test piece. The other end of the test piece is connected via the tension head and bridge to the centre of a precisely ground spring beam. The deflection of this spring-beam, which is supported on rollers, is transmitted through a simple lever system to a mercury piston which displaces mercury in a uniform bore glass tube, thus magnifying the beam deflection and providing an easily read scale of load. The advance of the mercury column is followed manually by the cursor and its attached needle which is used to puncture the graph sheet at frequent intervals; thus recording force. The movement of the worm gear which causes the test piece to elongate is transmitted through a gear train to the recording drum, the rotation of which is proportional to the elongation of the test piece. The resultant graph produced by joining successive punctures shows the load against the cross-head movement which is virtually a true stress/strain diagram from which the modulus of elasticity and tensile strength of the material could be determined. The force will then be recorded and the area of the cross-section's test piece, the mechanical properties are determined such as tensile strength, ultimate elongation and modulus of elasticity.

2.5.2 Impact test

The impact properties such as impact strength and impact energy of the composite sheet were tested in the civil engineering laboratory, university of Nigeria Nsukka (UNN), using a notch impact-testing machine. Force was applied to the composite sheet until it

fractured, and the impact strength was recorded. The impact strength of composite material is the fracture energy of the material.

3 Results and Discussions

Cross-sectional area of composite = 60.8mm^2

Average diameter of fibre = 0.41mm

Table 3.1. Mechanical Properties of OPEFBF Composites at Varying Volume Fractions and Aspect Ratios Using *Shape-Preserving-Linear-Interpolant* Type of Fitting to Obtain the Youngs' Modulus and Toughness.

S/N	Fibre volume fraction (%)	Fibre aspect ratio	Ultimate tensile strength (N/mm^2)	Ultimate elongation (mm)	Youngs' modulus (N)	Toughness (N/mm^2)
1	10	24.39	7.40	0.0086	362.52	0.032
2	10	73.17	8.31	0.011	514.00	0.048
3	10	121.95	6.58	0.012	133.00	0.047
4	30	24.39	10.77	0.0013	1198.60	0.074
5	30	73.17	13.98	0.022	738.026	0.170
6	30	121.95	6.17	0.020	908.05	0.100
7	50	24.39	4.77	0.013	805.44	0.044
8	50	73.17	4.95	0.013	1028.00	0.040
9	50	121.95	4.11	0.017	370.68	0.048

3.1.1 Tensile Test Results

Table 3.2 Analysis of Variance Result for Ultimate Tensile Strength

Source	Sum sq.	d.f.	Mean square	F	Prob>F
X1	48.66	2	24.33	6.67	0.053
X2	18.13	2	9.06	2.48	0.19
Error	14.60	4	3.65		
Total	81.38	8			

From Table 3.2, the ANOVA results of tensile strength, it is seen that the prob>F value for fibre volume fraction (X1) of 0.0532 falls within the acceptable range (≤ 0.05), thus the fibre volume fraction is a significant factor at 95% confidence bound. In comparison with the aspect ratio, fibre volume fraction has a more significant effect on the ultimate tensile strength of the composites. Figure 3.1 reveals that there is an increase in the ultimate tensile strength up to an optimum after which there was a corresponding decrease. Circular contour lines from the plot imply that factors significantly affect the property tested and that the optimum so obtained is a global optimum so improvement may not be possible. The coefficient of determination (R^2) obtained was 0.8207, implying 82% variability of ultimate tensile strength as shown in Table 3.3.

The ultimate tensile strength of the polyester laminate is 48N/mm^2 so from the results it can be seen that the addition of fibres to the resin reduced the tensile properties. However, the young's modulus which is about $400\text{-}1000\text{N/mm}^2$ increased to 1500N/mm^2 after the addition of fibres, which implies that added fibres to the polyester resin increased the young's modulus and reduced the tensile strength.

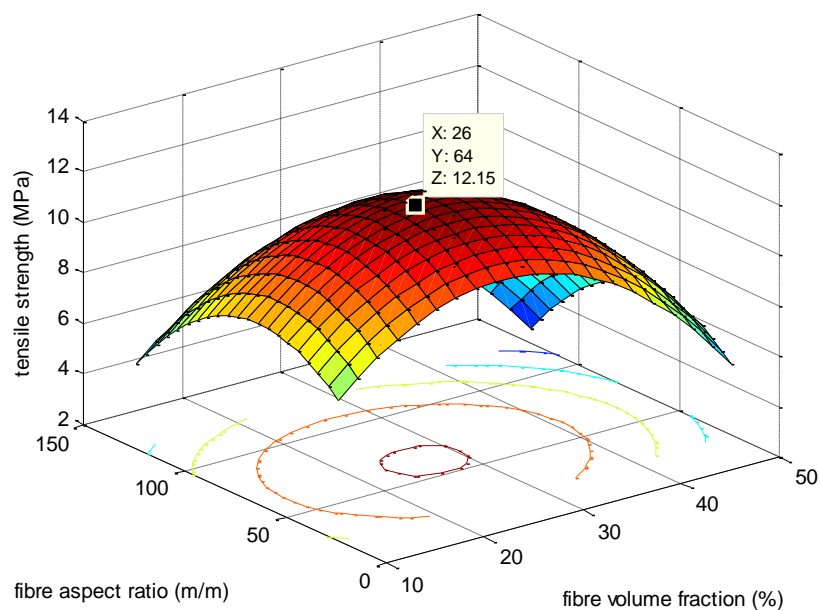


Figure 3.1. 3D plot of tensile strength versus fibre aspect ratio versus fibre volume fraction

Table 3.3. Numerical Results for Model Fit to Experimental Data for Tensile Strength

Variable	Coefficient	Standard Error	T Stat	P-Val	F Stat
Constant	0.42	3.50	0.12	0.91	Sse=14.594
X1	0.57	0.21	2.77	0.050	Dfe=4
X2	0.13	0.084	1.53	0.20	Dfr=4
X1²	-0.011	0.0034	-3.17	0.034	F=4.576
X2²	-0.0010	0.00057	-1.81	0.14	P-val=0.084953
	R ² =0.8207	AdjR ² =0.6413			

$$y=0.42381+0.5725*x1+0.12962*x2-0.010716*x1^2-0.0010277*x2^2$$

Where y is the ultimate tensile strength, x1 is the fibre volume fraction and x2 is the fibre aspect ratio.

The optimum tensile strength of 12.15 N/mm² occurred at a fibre volume fraction of 26% and fibre aspect ratio of 64m/m as can be seen from the surface plot.

3.1.2 Ultimate Elongation

Table 3.4 Analysis of Variance Result for Ultimate Elongation

Source	Sum sq.	d.f.	Mean square	F	Prob>F
X1	0.000030	2	1.50044e-005	0.41	0.6886
X2	0.00013	2	6.59244e-005	1.8	0.2767
Error	0.00015	4	3.65828e-005		
Total	0.00031	8			

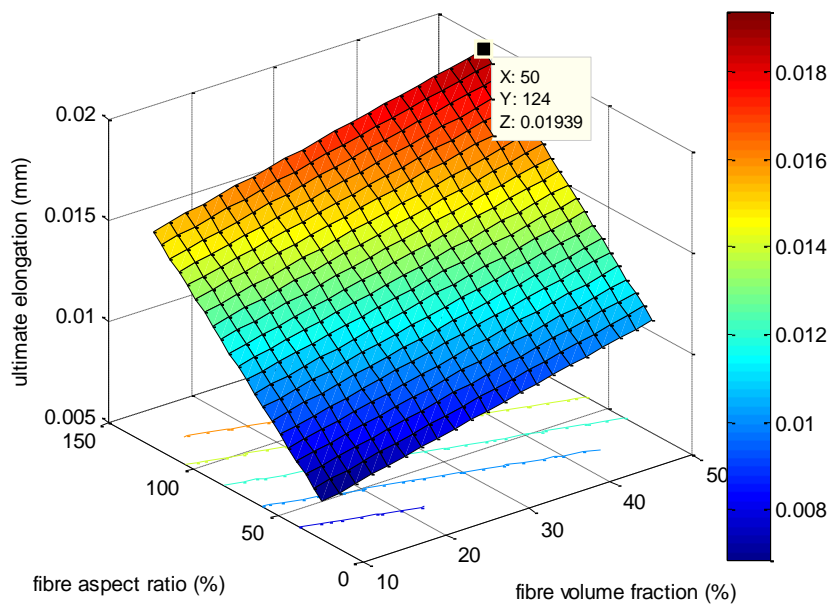


Figure 3.2 3D plot of ultimate elongation vs. fibre aspect ratio and volume fraction

From Table 3.4 ANOVA results for ultimate elongation, it can be seen that the prob>F values for both fibre volume fraction and fibre aspect ratio were greater than 0.1 (90% confidence) suggesting that both factors do not affect significantly the ultimate elongation. In fig 3.2, the contour lines which are parallel indicate that factors do not have a good interaction between them. The P values from t-stats and f-stats in table 3.5 indicate

the same as they didn't fall within the acceptable range of 0.1-0.01(90%-99%) confidence bounds.

Table 3.5. Numerical Results for Model Fit to Experimental Data for Ultimate Elongation

Variable	Coefficient	Standard Error	T Stat	P-Val	F Stat
Constant	0.0038	0.0050	0.75	0.48	Sse=0.000176
X1	0.000093	0.00011	0.84	0.43	Dfe=6
X2	0.000088	0.000045	1.94	0.10	Dfr=2
R²=0.4278	Adj R ² =0.2371			P-val=0.18733	

$$y=0.0038+0.0000933*x1+0.0000881*x2$$

x1 is fibre volume fraction; x2 is fibre aspect ratio, and y is ultimate elongation

The optimum ultimate elongation occurred at 0.01939 at a fibre volume fraction of 50, and fibre aspect ratio of 124 as can be seen from the surface plot.

3.1.3 Young's Modulus Results

Table 4.6 Analysis of Variance Result for Young's Modulus

Source	Sum sq.	d.f.	Mean sq.	F	Prob>F
X1	578352.9	2	289176.5	5.26	0.0758
X2	185903	2	92951.5	1.69	0.2934
Error	219717.9	4	54929.5		
Total	983973.8	8			

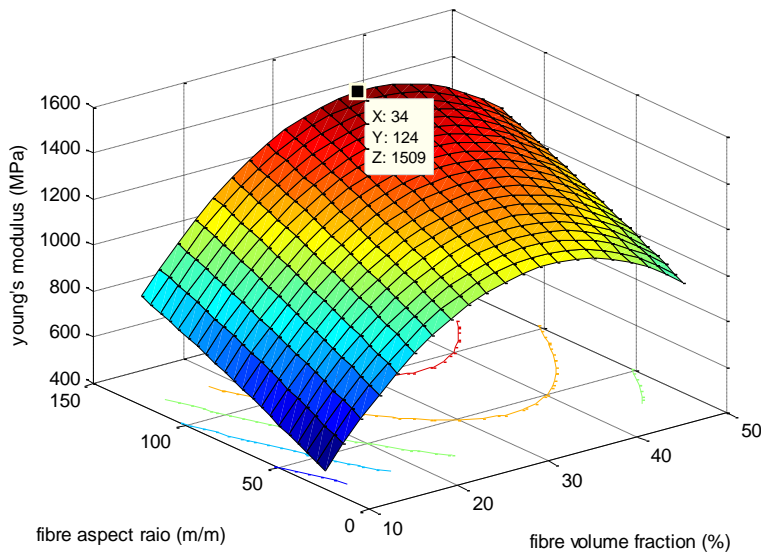


Figure 3.3. 3D-plot of Young modulus versus fibre aspect ratio versus fibre volume fraction.

Table 3.6 indicated that the fibre volume fraction played a more significant role in affecting Young’s modulus of elasticity than fibre aspect ratio based on their prob>F values. From table 3.7 the P-value for t-stats for volume fraction is less than 0.05 which indicates as well how significant a role fibre volume fraction played in the values of Young’s modulus of OPF composites. Fig 3.3, indicated that from the contour lines, there was a good interaction between the factors. R^2 of 0.7767 obtained implied a 78% variability of Young’s modulus.

Table 3.7. Numerical Results for Model Fit to Experimental Data for Young’s Modulus

Variables	Coefficients	Standard error	T stat	P-val	Fstat
Constants	-246.41	430.12	-0.57	0.60	Sse=2.19e-005
X1	71.85	25.31	2.84	0.047	Dfe=4
X2	4.75	10.38	0.46	0.67	Dfr=4
X1²	-1.031	0.41	-2.49	0.068	F=3.4784
X2²	-0.055	0.069	-0.79	0.48	P-val=0.12732

R2=0.7767 Adjusted R2=0.5534

$$y = -246.41 + 71.848 * x_1 + 4.7508 * x_2 - 1.0315 * x_1^2 - 0.0054756 * x_2^2;$$

x1 is fibre volume fraction; x2 is the fibre aspect ratio, and y is the young's modulus

Optimum occurred at a fibre volume fraction of 34 and a fibre aspect ratio of 124.

Optimum Young's modulus is obtained as $1509\text{N/mm}^2 = 1500\text{N/mm}^2$

3.1.4 Toughness

Table 3.8 Analysis of Variance Result for Toughness

Source	Sum sq.	d.f.	Mean square	F	Prob>F
X1	0.011	2	0.0057	4.39	0.098
X2	0.00081	2	0.0004	0.3	0.75
Error	0.0052	4	0.0013		
Total	0.017	8			

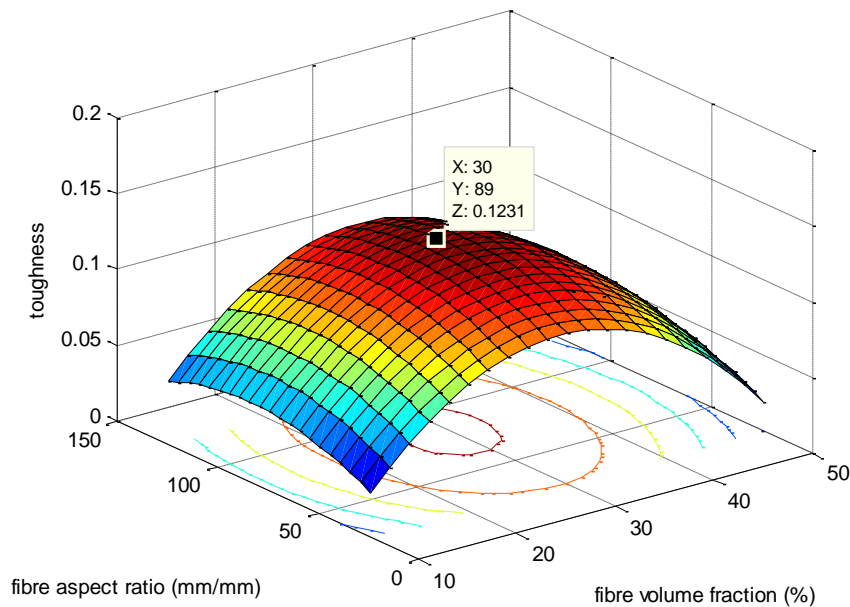


Figure 3.4 3D-plot of toughness versus fibre aspect ratio versus fibre volume fraction

Tables 3.8 and 3.9 showed that the aspect ratio played a more significant role in the toughness of the composites based on their P-value from t-stats and the ANOVA table. Fig 3.4 revealed a quadratic increase in the toughness until optimum was obtained after

which there was a corresponding decrease. The circular contour lines in the plot indicated a good interaction between factors. In addition, the circular contour line indicated a global optimum so an improvement on the optimum may not be possible. R^2 value of 0.7015 obtained indicated 70% variability in the toughness of the composites.

Table 3.9. Numerical Results for Model Fit to Experimental Data for Toughness

Variables	Coefficients	Standard error	T stat	P-value	Fstat
Constants	-0.085	0.066	-1.28	0.27	Sse=0.0052198
X1	0.011	0.0039	2.83	0.048	Dfe=4
X2	0.0011	0.0016	0.70	0.52	Dfr=4
X1²	-0.00018	-0.000064	-2.94	0.042	F=2.3501
X2²	-0.0000067	0.000011	-0.62	0.57	P-val=0.21412
R²=0.7015	AdjR²=0.4030				

$$y = -0.085091 + 0.011027 * x_1 + 0.0011183 * x_2 - 0.00018798 * x_1^2 - 0.0000066892 * x_2^2$$

x_1 is fibre volume fraction; x_2 is fibre aspect ratio.

Optimum occurred at a fibre volume fraction of 30 and a fibre aspect ratio of 89.

Optimum toughness is obtained as 123.1N/mm².

For the rational type of fitting, Tables 3.11 and 3.12 indicated in correspondence to the values obtained above that the fibre volume fraction played a more significant role than the aspect ratio. However, in comparison, the optimum obtained here is higher than that obtained previously, which indicates a better model fit with rational (linear-quadratic fitting).

Moreso, from tables 3.13 and 3.14, fibre volume fraction had a more significant effect on Young's modulus of elasticity based on their respective values from ANOVA and t-stats and f-stats. An R^2 value of 0.9247 was obtained showing a better fit when compared to that obtained from a linear fit.

Table 3.10 Mechanical Properties of OPEFBF Composites at Varying Volume Fractions and Aspect Ratios using *Rational* Type of Fitting to Obtain the Youngs’ Modulus and Toughness.

S/N	Fibre volume fraction (%)	Fibre aspect ratio	Ultimate tensile strength (N/mm ²)	Ultimate elongation (mm)	Youngs’ modulus (N)	Toughness (N/mm ²)
1	10	24.39	7.40	0.0086	523.012	0.032
2	10	73.17	8.31	0.011	616.43	0.048
3	10	121.95	6.58	0.012	884.19	0.048
4	30	24.39	10.77	0.0013	831.36	0.072
5	30	73.17	13.98	0.022	800.35	0.17
6	30	121.95	6.17	0.020	958.075	0.16
7	50	24.39	4.77	0.013	879.98	0.043
8	50	73.17	4.95	0.013	935.54	0.040
9	50	121.95	4.11	0.020	837.20	0.063

For the impact test, tables 3.15 and 3.16 showed that both fibre aspect ratio and fibre volume fraction played a very important role as their P-value are less than 0.05 (95% confidence bounds). Fig 3.7 showed a quadratic increase in impact energy up to optimum after which there was a corresponding decrease. The circular contour lines indicated a good interaction between the factors and a global optimum-improvement may not be possible. An R² value of 0.9373 was obtained which implied a good model fit and a 94% variability of the impact energy.

Also, from tables 3.17 and 3.18, the P-value indicated that both fibre volume fraction and fibre aspect ratios significantly affect the impact strength of the composites. The 3-D plot of fig 3.8 showed oval contour lines indicating a good interaction between the factors and a global optimum i.e there may not be a possible improvement on it. An R² value of 0.9117 obtained implies a good model fit and a 91% variability of impact strength.

3.1.5 Toughness

Table 3.11 Analysis of Variance Result for Toughness

Source	Sum sq.	d.f.	Mean square	F	Prob>F
X1	0.018	2	0.0091	7.13	0.048
X2	0.0028	2	0.0014	1.1	0.415
Error	0.0051	4	0.0013		
Total	0.026	8			

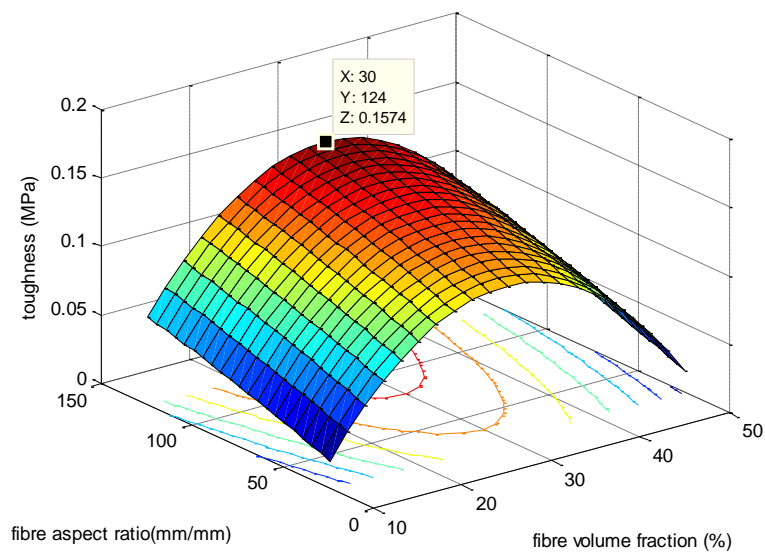


Figure 3.5 3D-plot of toughness versus fibre aspect ratio versus fibre volume fraction for rational model

Table 3.12. Numerical Results for Model Fit to Experimental Data for Toughness

Variables	Coefficients	Standard error	T stat	P-value	Fstat
Constants	-0.11	0.066	-1.69	0.17	Sse=0.0052146
X1	0.014	0.0039	3.67	0.021	Dfe=4
X2	0.00058	0.0016	0.36	0.73	Dfr=4
X1²	-0.00024	-0.000063	-3.77	0.020	F=4.1167
X2²	-0.00000091	0.000011	-0.086	0.94	P-val=0.099658
R²=0.8046	AdjR²=0.61				

$$y = -0.11124 + 0.014174 * x_1 + 0.00057795 * x_2 - 0.000238 * x_1^2 - 0.000000911 * x_2^2$$

x_1 is fibre volume fraction; x_2 is the fibre aspect ratio, and y is the toughness

Optimum occurred at a fibre volume fraction of 30 and a fibre aspect ratio of 124.

Optimum toughness is obtained as 157.4 N/mm^2

3.1.6 Young's Modulus Results

Table 3.13 Analysis of Variance Result for Young's Modulus

Source	Sum sq.	d.f.	Mean sq.	F	Prob>F
X1	80333.5	2	40166.8	3.02	0.1585
X2	35795.6	2	17897.8	1.35	0.357
Error	53137.4	4	13282.4		
Total	169266.6	8			

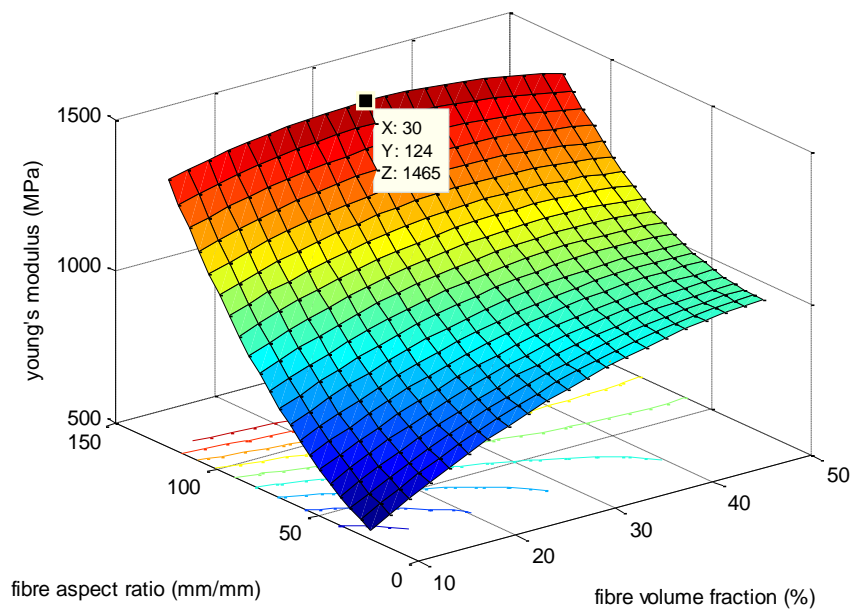


Figure 3.6 3D-plot of Young modulus versus fibre aspect ratio versus fibre volume fraction for rational model

Table 3.14. Numerical Results for Model Fit to Experimental Data for Young’s Modulus

Variables	Coefficients	Standard error	T stat	P-value	Fstat
Constants	235.38	140.30	1.68	0.19	Sse=12745
X1	25.33	7.45	3.40	0.042	Dfe=3
X2	2.45	3.10	0.80	0.480	Dfr=5
X1X2	-0.10	0.033	-3.08	0.054	F=7.3688
X1²	-0.21	0.12	-1.81	0.17	Pval=0.065459
X2²	0.015	0.019	0.76	0.50	
R²=0.9247	AdjR²=0.7992				

$$y=235.3800+25.3260*x_1+2.4531*x_2-0.1030*x_1*x_2-0.2088*x_1^2+0.04791*x_2^2$$

where y is young’s modulus, and x1 is fibre volume fraction; x2 is the fibre aspect ratio.

Optimum occurred at a fibre volume fraction of 30 and a fibre aspect ratio of 124.

Optimum Young’s modulus is obtained as 146.5N/mm²

3.1.7 Impact Energy Test

Table 3.15 Analysis of Variance Results for Impact Energy

Source	Sum sq.	d.f.	Mean sq.	F	Prob>F
X1	9.07	2	4.53	19.98	0.0083
X2	4.50	2	2.25	9.92	0.0282
Error	0.91	4	0.23		
Total	14.47	8			

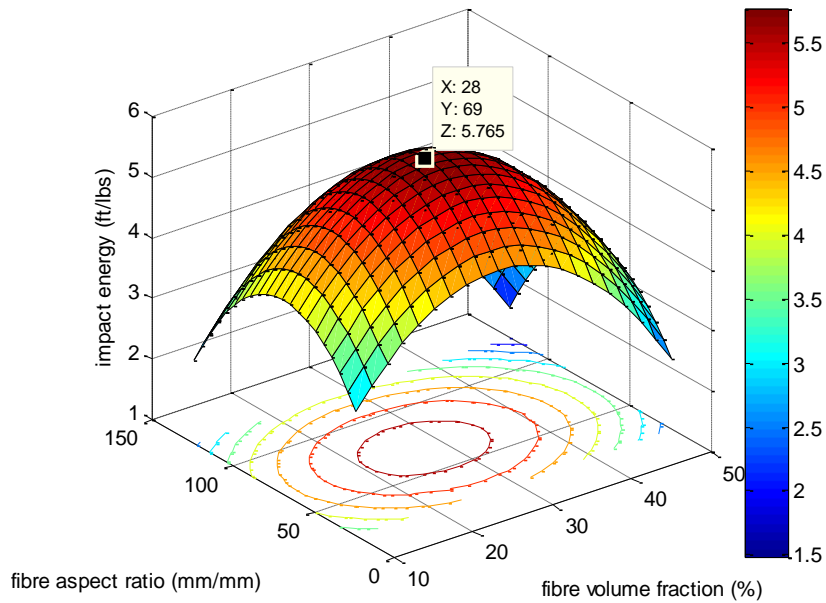


Figure 3.7 3D-plot of Impact energy versus fibre aspect ratio and fibre volume fraction

Table 3.16: Numerical Results for Model Fit to Experimental Data for Impact Energy

Variables	Coefficients	Standard error	T stat	P-value	Fstat
Constants	-0.78	0.87	-0.90	0.42	Sse=0.90738
X1	0.27	0.051	5.28	0.0062	Dfe=4
X2	0.081	0.021	3.86	0.018	Dfr=4
X1 ²	-0.0049	0.00084	-5.84	0.0043	F= 14.9486
X2 ²	-0.00059	0.00014	-4.21	0.014	P-val=0.0113
R²= 0.9373		AdjR²=0.8746			

$$y = -0.7827 + 0.2718 * x_1 + 0.0814 * x_2 - 0.0049 * x_1^2 - 0.0005960 * x_2^2$$

where y is the impact energy, and x1 is fibre volume fraction; x2 is the fibre aspect ratio.

The optimum 307.72J/m (5.77ft-lbs/in) occurred at a fibre volume fraction of 28, and an aspect ratio of 69 as can be seen from the surface plot.

3.1.8 Impact Strength Test Results

Table 3.17 Analysis of Variance Result for Impact Strength

Source	Sum sq.	d.f.	Mean sq.	F	Prob>F
X1	0.23	2	0.12	15.13	0.0136
X2	0.084	2	0.042	5.53	0.0705
Error	0.030	4	0.0076		
Total	0.35	8			

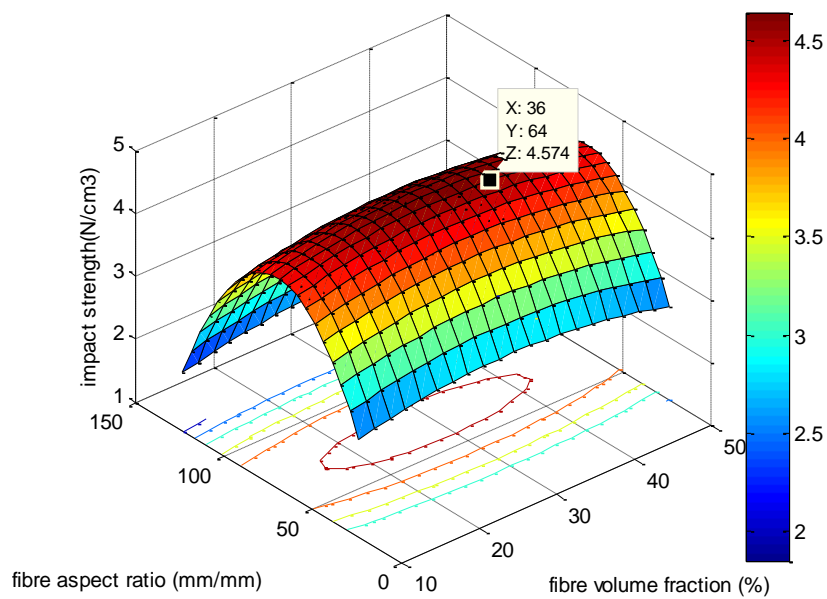


Figure 3.8 3D-plot of Impact strength versus fibre aspect ratio versus fibre volume fraction

Table 3.18. Numerical Results for Model Fit to Experimental Data for Impact Strength

Variables	Coefficients	Standard error	T stat	P-value	Fstat
Constants	-0.20	0.16	-1.27	0.27	Sse=0.0305
X1	0.049	0.0094	5.16	0.0067	Dfe=4
X2	0.012	0.0038	3.04	0.038	Dfr=4
X1 ²	-0.00084	0.00015	-5.43	0.0056	F= 10.33
X2 ²	-0.00084	0.000025	- 3.24	0.032	P-val=0.0220
R²= 0.9117 AdjR²=0.8235					

$$y = -0.2029 + 0.0487 * x_1 + 0.118 * x_2 - 0.0008375 * x_1^2 - 0.0008405 * x_2^2;$$

where y is the impact strength and x1 is fibre volume fraction; x2 is the fibre aspect ratio. The optimum 0.046N/mm² occurred at a fibre volume fraction of 36, and a fibre aspect ratio of 64 as can be seen from the surface plot.

Mean energy absorption capacity is given as s

$$U = \frac{A_{max}^2 \times A_0}{E_{mean}}$$

Where

A_{max} = maximum breaking stress of the sample

A₀ = original length of the sample = 160mm = 0.16m

E_{mean} = Mean Young modulus of elasticity calculated

$$E_{mean} = \frac{362.52 + 514 + 133 + 1198.6 + 738.0256 + 908.05 + 805.44 + 1028 + 370.6796}{9} = 673.15 \text{ N/mm}^2$$

$$= 673.15 * 10^6 \text{ N/m}^2$$

Mean energy absorption capacity is, therefore;

$$U_m = \frac{U_1 + U_2 + \dots + U_9}{9}$$

$$U_m = 0.2 \text{ J}$$

4 Conclusion

This project work is based on modelling the mechanical properties of OPR composites was done and the properties tested here include ultimate tensile strength, toughness, Young's modulus, impact strength and impact energy. Based on the results, optimization was carried out and the optimum value for each property tested was determined.

From this work, it was found that the fibre volume fraction significantly affects the properties more than the aspect ratio. For ultimate tensile strength optimization that the optimum obtained was a global one at fibre volume fraction and aspect ratio of 26% and 64 respectively. The optimum ultimate tensile strength was 12.15N/mm². For Young's modulus, optimization revealed that at a fibre volume fraction of 34% and aspect ratio of 124, the optimum value for Young's modulus was obtained to be 1509 N/mm².

For toughness, the optimization carried out showed an optimum value of 0.1231 N/mm² at a fibre volume fraction of 30% and an aspect ratio of 89. For the rational (linear-quadratic) type of fitting, the optimum obtained for toughness was 0.16 N/mm² at a fibre volume fraction of 30% and aspect ratio of 124. Also, the optimum obtained here for Young's modulus was found to be 1465 N/mm² at a 30% volume fraction and an aspect ratio of 124. For impact strength, optimization indicated a global optimum at values of aspect ratio and fibre volume fraction of 69 and 28% respectively. An optimum value of impact strength of 307.72J/m (5.77ft/lbs) was obtained.

Acknowledgements

I want to specially acknowledge Engr. Dr Emmanuel C. Osoka for his relentless effort in guiding and supervising this work and ensuring I conduct resourceful research.

References

- [1] R. M. Guedes and J. Xavier “Understanding and Predicting Stiffness in Advanced Fibre-Reinforced Polymer (FRP) Composites for Structural Applications”, In *Advanced Fibre-Reinforced Polymer (FRP) Composites for Structural Applications* (pp. 298-360). Woodhead Publishing. 2013.
- [2] J. P. Jose, S. Thomas, J. Kuruvilla, S. K. Malhotra, K. Goda, M. S. Sreekala, “Advances in Polymer Composites: Macro-and Microcomposites—State of The Art, New Challenges, and Opportunities”, *Polymer composites*, **1**, 3-16. 2012.
- [3] J. Kuruvilla, R. D. Toledo Filho, J. Beena, T. Sabu, and L. H. Carvalho, “A Review on Sisal Fiber Reinforced Polymer Composites”, *Revista Brasileira de Engenharia Agrícola e Ambiental*, **3**(3), 367-379. 1999.
- [4] X. Li, L. G. Tabiland, S. Panigrahi, “Chemical Treatments of Natural Fibre for Use in Natural Fibre-Reinforced Composites: A Review, *Journal of Polymers and the Environment*”, **15**(1), 25-33. 2007.
- [5] S.M. Lee, D. Cho, W.H. Park, S.G. Lee, S.O. Han, and L.T. Drzal, “Novel Silk/Poly (Butylene Succinate) Biocomposites: The Effects of Short Fibre Content on their Mechanical and Thermal Properties”, *Composites Science and Technology*, **65**, 647-657. 2005.
- [6] H. Y. Cheung, M. P. Ho, K. T. Lau, F. Cardona, and D. Hui, “Natural Fibre-Reinforced Composites for Bioengineering and Environmental Engineering Applications”, *Composites Part B: Engineering*, **40**(7), 655-663. 2009.
- [7] E. C. Osoka and O. D. Onukwuli, *The Optimum Condition for Mercerization of Oil Palm Empty Fruit Bunch Fibre*, *International Journal of Innovative Research in Computer Science and Technology*, **3**(4), 50-56. 2015.
- [8] D. Jones, G. O. Ormondroyd, S. F. Curling, C. M. Popescu, and M. C. Popescu, “Chemical Compositions of Natural Fibres. In *Advanced High Strength Natural Fibre Composites in Construction*”, (pp. 23-58), Woodhead Publishing, 2017.
- [9] M. Y. Hashim, A. M. Amin, O. M. F. Marwah, M. H. Othman, M. R. M. Yunus, and N. C. Huat, “The Effect of Alkali Treatment Under Various Conditions On

- Physical Properties of Kenaf Fibre”, In *Journal of Physics: Conference Series* **914**(1), 012030. IOP Publishing, 2017.
- [10] A. K. Mohanty, M. Misra, and L. T. Drzal, “Surface Modifications of Natural Fibres and Performance Of The Resulting Biocomposites: An Overview”, *Composite interfaces*, **8**(5), 313-343. 2001
- [11] A. Bismarck, A. K. Mohanty, I. Aranberri-Askargorta, S. Czapla, M. Misra, G. Hinrichsen and J. Springer. “Surface Characterization of Natural Fibres; Surface Properties and The Water Up-Take Behavior of Modified Sisal and Coir Fibres”, *Green chemistry*, **3**(2), 100-107. 2001
- [12] L. A. Pothan, J. George, & S. Thomas, “Effect of Fibre Surface Treatments on the Fibre–Matrix Interaction in Banana Fibre Reinforced Polyester Composites”, *Composite Interfaces*, **9**(4), 335-353. 2002.
- [13] N. T. Phuong, C. Sollogoub and A. Guinault, “Relationship Between Fibre Chemical Treatment and Properties of Recycled Pp/Bamboo Fibre Composites”, *Journal of Reinforced Plastics and Composites*, **29**(21), 3244-3256. 2010
- [14] T., Padmavathi, S. V. Naidu & R. M. V. G. K. Rao. “Studies On Mechanical Behavior of Surface Modified Sisal Fibre–Epoxy Composites”, *Journal of Reinforced Plastics and Composites*, **31**(8), 519-532. 2012.
- [15] Petinakis, E., Yu, L., Simon, G., & Dean, K. (2013). “Natural Fibre Bio-Composites Incorporating Poly (Lactic Acid)”, *Fibre reinforced polymers-The technology applied for concrete repair*, 41-59. 2013.
- [16] O. Faruk, A. K. Bledzki, H. P. Fink & M. Sain, “Biocomposites Reinforced with Natural Fibres: 2000–2010”, *Progress in polymer science*, **37**(11), 1552-1596. 2012.
- [17] M. Y. Hashim, A. Zaidi, A. Mujahid, & S. Ariffin, “Plant Fiber Reinforced Polymer Matrix Composite: A Discussion On Composite Fabrication and Characterization Technique”. In *Seminar to Faculty of Civil and Environmental Engineering (FKAAS)*, Universiti Tun Hussein Onn Malaysia (UTHM). 2012.

- [18] C. M. Ewulonu and , I. O. Igwe. “Properties of Oil Palm Empty Fruit Bunch Fibre Filled High Density Polyethylene”. *International journal of engineering and technology*, **3**(6), 2012.
- [19] A., Athijayamani, M. Thiruchitrambalam, V. Manikandan and B. Pazhanivel, “Mechanical Properties of Natural Fibers Reinforced Polyester Hybrid Composite”, *International Journal of Plastics Technology*, **14**(1), 104-116. 2010.
- [20] S. M. Sapuan, A. Leenie, M. Harimi, and Y. K. Beng, “Mechanical Properties of Woven Banana Fibre Reinforced Epoxy Composites”. *Materials & design*, **27**(8), 689-693. 2006.
- [21] F. K. A. Nugraha, “Shrinkage of Biocomposite Material Specimens [HA/Bioplastic/Serisin] Printed using a 3D Printer using the Taguchi Method”, *International Journal of Applied Sciences and Smart Technologies*, **4**(1), 89-96. 2022.

This page intentionally left blank